Acta Crystallographica Section B
Structural Science
ISSN 0108-7681

Pressure-induced phase transitions in L-alanine, revisited

N. A. Tumanov,[a] E. V. Boldyreva,[a,b]* B. A. Kolesov,[a,c] A. V. Kurnosov[a,c] and R. Quesada Cabrera[d,e]

[a]Novosibirsk State University, REC-008, Pirogova 2, Novosibirsk 90, Russia, [b]Institute of Solid State Chemistry and Mechanochemistry SB RAS, Kutateladdze 18, Novosibirsk 128, Russia, [c]Nikolaev Institute of Inorganic Chemistry SB RAS, Lavrent'eva 3, Novosibirsk 90, Russia, [d]Swiss–Norwegian Beamline ESRF, Grenoble, rue Jules Horowitz, BP220, Grenoble CEDEX, France, and [e]University College London, Christopher-Ingold Laboratories, 20 Gordon Street, London WC1H 0AJ, England

Correspondence e-mail: eboldyreva@yahoo.com

Received 19 January 2010
Accepted 26 May 2010

The effect of pressure on L-alanine has been studied by X-ray powder diffraction (up to 12.3 GPa), single-crystal X-ray diffraction, Raman spectroscopy and optical microscopy (up to ~6 GPa). No structural phase transitions have been observed. At ~2 GPa the cell parameters *a* and *b* become accidentally equal to each other, but without a change in space-group symmetry. Neither of two transitions reported by others (to a tetragonal phase at ~2 GPa and to a monoclinic phase at ~9 GPa) was observed. The changes in cell parameters were continuous up to the highest measured pressures and the cells remained orthorhombic. Some important changes in the intermolecular interactions occur, which also manifest themselves in the Raman spectra. Two new orthorhombic phases could be crystallized from a MeOH/EtOH/H_2O pressure-transmitting mixture in the pressure range 0.8–4.7 GPa, but only if the sample was kept at these pressures for at least 1–2 d. The new phases converted back to L-alanine on decompression. Judging from the Raman spectra and cell parameters, the new phases are most probably not L-alanine but its solvates.

1. Introduction

Polymorphism of amino acids is intensively studied because of the importance of these compounds as materials, drugs and biomimetics (Boldyreva, 2007*a*,*b*,*c*, 2008, 2009; Moggach *et al.*, 2008). L-Alanine is one of the first crystalline amino acids to be studied at high pressure, and a phase transition has been reported to take place at 2.3 GPa (Teixeira *et al.*, 2000). In 2006 we carried out an angle-dispersive high-resolution X-ray powder diffraction study at ESRF, but could not find any confirmation of a structural phase transition, at least up to 8.5 GPa, the highest pressure reached in that experiment. By the time our data were processed and ready for publication, two other papers reporting a phase transition in L-alanine into a tetragonal phase at 2.3 GPa and a monoclinic phase at 9 GPa had been published. The conclusions from these phase transitions were based on an energy-dispersive X-ray powder diffraction study at the HASYLAB-DESY synchrotron source (Olsen *et al.*, 2006, 2008). The orthorhombic-to-tetragonal symmetry change reported at 2.3 GPa requires an enormous structural re-arrangement, which is difficult to imagine. Since neither the space-group symmetry nor the atomic coordinates of the high-pressure polymorphs have been reported, we have undertaken one more structural study of the system, this time using single-crystal diffraction. The changes in cell parameters and volume reported in our powder and single-crystal experiments agreed well, and the single-crystal diffraction study confirmed the conclusions (based on our own powder-diffraction experiments) that no structural

phase transition occurs in the range studied. Although the diamond–anvil cell (DAC) allowed us to increase pressure further, the high-quality single-crystal diffraction experiment was no longer possible above 3.5 GPa on a slow step-wise compression, because of the partial recrystallization of the crystal into a polycrystalline sample (see §3). However, single-crystal diffraction data at 3.9, 4.7 and 5.9 GPa could be collected in another experiment, when the crystal of L-alanine was quickly compressed up to 5.9 GPa. In this case the crystallization only started on slow reverse decompression at $\sim$ 4.7 GPa. To check the occurrence of the second reported phase transition, once again we carried out an angle-dispersive X-ray powder diffraction study at ESRF, this time aiming at the higher pressure range. No changes in space-group symmetry were observed at least up to 12.3 GPa (the highest pressure reached in the experiment).[1] Since the conclusion on the pressure-induced phase transition at 2.3 GPa in L-alanine was originally based on Raman measurements (Teixeira *et al.*, 2000), we also re-measured the Raman spectra of L-alanine at high pressures to see if the previously reported spectroscopic data could be reproduced. The observations reported by Teixeira *et al.* (2000) have been reproduced, in general, but we could not correlate them with a structural phase transition, only with subtle continuous changes in the intermolecular interactions.

The present paper serves as an illustration of how a combination of X-ray diffraction, Raman spectroscopy and optical microscopy can provide an insight into subtle pressure-induced changes in the amino acid crystals not necessarily related to any polymorphic transformations. It also provides one more example that the effect of pressure on the same sample can differ, depending on the rate at which the same pressure value was reached (Boldyreva, 2007*b*): L-alanine does not undergo any structural phase transitions when compressed and decompressed quickly, but forms solvates with MeOH/EtOH/water, if kept in the pressure range 0.8–4.7 GPa for a long time, converting back to L-alanine on decompression.

2. Experimental

L-Alanine was purchased from Sigma–Aldrich (Vienna, Austria). Small crystals of good quality for single-crystal experiments could be selected from the batch; for the experiments with powder, the sample was gently ground. In the first series of powder diffraction experiments hydrostatic pressure was created in a modified Merrill–Bassett diamond–anvil cell (DAC) without Be supports (Ahsbahs, 2004; Sowa & Ahsbahs, 2006; gasket material Thyrodur-2709, starting thickness 0.180 mm, pre-indented to 0.104 mm and then hardened by heating at 773 K over 6 h in micronized iron oxide and subsequent cooling; hole diameter 0.3 mm; Ahsbahs, 1996). In the second series of powder diffraction experiments we used an ETH-type DAC (Allan *et al.*, 1996; stainless steel gasket, starting thickness 0.200 mm, pre-indented to 0.055 mm, hole diameter 0.3 mm). Boehler–Almax DACs (Boehler, 2006) were used in single-crystal diffraction and Raman spectroscopy experiments (stainless steel gasket, starting thickness 0.200 mm, pre-indented to 0.120 mm, hole diameter 0.3 mm). In all the experiments, pressure was estimated from the shift in the R1 band of a ruby calibrant ($\pm$0.05 GPa; Forman *et al.*, 1972; Piermarini *et al.*, 1975). A methanol–ethanol (4:1) mixture [(quasi)hydrostatic limit 10.4 GPa; Piermarini *et al.*, 1973] was used as the pressure-transmitting liquid in the first series of powder diffraction experiments; a methanol–ethanol–water (16:3:1) mixture [(quasi)hydrostatic limit 14.5 GPa; Fujishiro *et al.*, 1981] was used in the second series of powder diffraction experiments, when we aimed at higher pressures. Both methanol–ethanol and methanol–ethanol–water mixtures were used in different series of single-crystal diffraction experiments.

High-resolution X-ray powder diffraction experiments were carried out using a synchrotron radiation source (λ = 0.7014 Å in the first series of experiments, λ = 0.70007 Å in the second, λ = 0.700027 Å in the extra powder diffraction experiments aimed at identifying the polycrystalline phases which crystallized under special conditions and co-existed with the original single-crystal of L-alanine, see §3). Diffraction patterns were registered using a MAR345 two-dimensional image-plate detector at the BM1A station at the Swiss–Norwegian Beamline at ESRF in Grenoble. The frames were measured at 20 pressure points up to 8.5 GPa in the first series, at 8 pressure points up to 12.3 GPa in the second, and at 13 pressure points from 3.8 GPa down to ambient pressure when identifying the polycrystalline phase with exposure times of 600–7200 s. The sample-to-detector distance was $\sim$ 340 mm in the first series, 350 mm in the second and 300 mm when identifying the polycrystalline phase. Silicon powder was used for the calibration of the sample-to-detector distance.

Single-crystal X-ray diffraction experiments were carried out using an Oxford Diffraction Xcalibur Gemini diffractometer (Mo $K\alpha$ radiation, 0.5 mm collimator, graphite monochromator, ω-scan, scan step 0.3°, 12 s per frame) at 6 pressure points. Data were collected using *CrysAlis Pro* software (Oxford Diffraction, 2008*a*,*b*). We used the strategy described in Budzianowski & Katrusiak (2004), but slightly modified it to avoid goniometer collision of our instrument. We used the same strategy for all single-crystal experiments, only the time per frame was sometimes different. The completeness of the datasets was 43–59%, depending on the experiment. Initial crystal dimensions were 0.15 × 0.10 × 0.05 mm and 0.2 × 0.11 × 0.05 mm in the first and second series of experiments, respectively. During the first series of the single-crystal X-ray measurements at 1.5 GPa the sample in the cell shifted; the data collected before and after the shift were processed separately and then merged.

The raw powder diffraction data were processed (calibration, masking of the reflections from diamond and ruby, integration) using the program *Fit*2D (Hammersley *et al.*, 1996). Powder patterns were indexed using *DICVOL*06

[1] At 12.3 GPa the pressure-transmitting liquid became viscous and the diffraction lines started broadening. The last pressure point for which high-quality structural data were obtained was somewhat lower (10.4 GPa).

Table 1
Experimental details (single-crystal diffraction).

For all structures: $C_3H_7NO_2$, M_r = 89.10, orthorhombic, $P2_12_12_1$, Z = 4. Experiments were carried out at 293 K with Mo $K\alpha$ radiation using an Oxford Diffraction KM4 CCD diffractometer. Absorption was corrected for by numerical methods, *Absorb*6.1 (Angel, 2004). Refinement was with 0 restraints. H-atom parameters were constrained.

	0.2 GPa	0.8 GPa	1.5 GPa	2.2 GPa	2.9 GPa
Crystal data					
a, b, c (Å)	5.7952 (6), 5.933 (8), 12.362 (3)	5.7464 (5), 5.834 (5), 12.260 (2)	5.6999 (14), 5.772 (7), 12.161 (6)	5.6729 (7), 5.671 (2), 12.047 (5)	5.6254 (9), 5.573 (3), 11.942 (6)
V (Å^3)	425.0 (6)	411.0 (4)	400.1 (5)	387.5 (2)	374.3 (3)
μ (mm^{-1})	0.12	0.12	0.12	0.13	0.13
Crystal size (mm)	0.15 × 0.1 × 0.05	0.15 × 0.1 × 0.05	0.15 × 0.09 × 0.05	0.14 × 0.06 × 0.05	0.14 × 0.06 × 0.05
Data collection					
T_{min}, T_{max}	0.994, 0.994	0.994, 0.994	0.994, 0.994	0.992, 0.993	0.993, 0.994
No. of measured, independent and observed [$I > 2\sigma(I)$] reflections	2729, 372, 249	2584, 361, 248	2561, 707, 336	3618, 565, 318	3586, 564, 325
R_{int}	0.098	0.073	0.097	0.088	0.124
Refinement					
$R[F^2 > 2\sigma(F^2)]$, $wR(F^2)$, S	0.036, 0.086, 0.87	0.035, 0.079, 0.90	0.044, 0.094, 0.81	0.035, 0.085, 0.86	0.053, 0.114, 0.90
No. of reflections	372	361	707	565	564
No. of parameters	57	52	57	57	57
$\Delta\rho_{max}$, $\Delta\rho_{min}$ (e Å^{-3})	0.11, −0.12	0.13, −0.10	0.16, −0.20	0.13, −0.13	0.22, −0.18

	3.5 GPa	3.9 GPa	4.7 GPa	5.9 GPa
Crystal data				
a, b, c (Å)	5.6084 (7), 5.552 (2), 11.857 (4)	5.6083 (5), 5.5139 (14), 11.815 (3)	5.5845 (5), 5.4749 (19), 11.721 (3)	5.5441 (4), 5.4007 (12), 11.587 (2)
V (Å^3)	369.2 (2)	365.4 (2)	358.4 (2)	346.9 (1)
μ (mm^{-1})	0.13	0.14	0.14	0.14
Crystal size (mm)	0.14 × 0.06 × 0.05	0.2 × 0.11 × 0.05	0.2 × 0.11 × 0.05	0.2 × 0.11 × 0.05
Data collection				
T_{min}, T_{max}	0.993, 0.994	0.992, 0.993	0.992, 0.993	0.992, 0.993
No. of measured, independent and observed [$I > 2\sigma(I)$] reflections	3530, 544, 326	3567, 586, 388	2416, 492, 335	3335, 533, 402
R_{int}	0.136	0.084	0.075	0.062
Refinement				
$R[F^2 > 2\sigma(F^2)]$, $wR(F^2)$, S	0.046, 0.107, 0.89	0.040, 0.085, 0.94	0.034, 0.063, 0.89	0.031, 0.066, 0.94
No. of reflections	544	586	492	533
No. of parameters	57	57	57	57
$\Delta\rho_{max}$, $\Delta\rho_{min}$ (e Å^{-3})	0.20, −0.18	0.17, −0.17	0.16, −0.13	0.17, −0.18

Computer programs used: *CrysAlis Pro* (Oxford Diffraction Ltd, 2008*a*,*b*), *SHELXS*97, *SHELXL*97 (Sheldrick, 2008), *Mercury* (Macrae *et al.*, 2006), *CrystalExplorer* (Wolff *et al.*, 2007), *PLATON* (Spek, 2009).

(Boultif & Louër, 2004) and *WinXPOW* (Stoe & Cie, 2002) software. A search of indexing solutions was carried out among all crystal systems except triclinic. *DASH*3.1 software (David *et al.*, 2006) was used for structure solution with subsequent structure refinement by *GSAS* (Larson & Von Dreele, 1994).

Single-crystal data were reduced using *CrysAlis Pro* software. First of all, ~ 20–30 peaks from the sample were selected manually, and the unit cell and the orientation matrix were found. The peak-hunting procedure was then run, and the current unit cell was used to re-index the data (about 30% of all peaks could be indexed). Data were reduced as from a single-crystal sample, without taking diamond's reflections into account. The overlapping of the sample's and diamond's reflections was checked manually afterwards and the reflections affected excluded. Absorption by diamonds, the gasket and the crystal was corrected numerically using *Absorb*6.1 (Angel, 2004) software. The structures were solved and refined with standard *SHELX* (Sheldrick, 2008) procedures using the X-Step32 shell (Stoe & Cie, 2002). All non-H atoms were refined in the anisotropic approximation. H atoms were placed geometrically. TLS correction with *WinGX* (Farrugia, 1999) was attempted, but had no significant effect on the trends observed, although of course it did affect the absolute values of the interatomic distances. Experimental details and refinement parameters are given in Table 1 for the single-

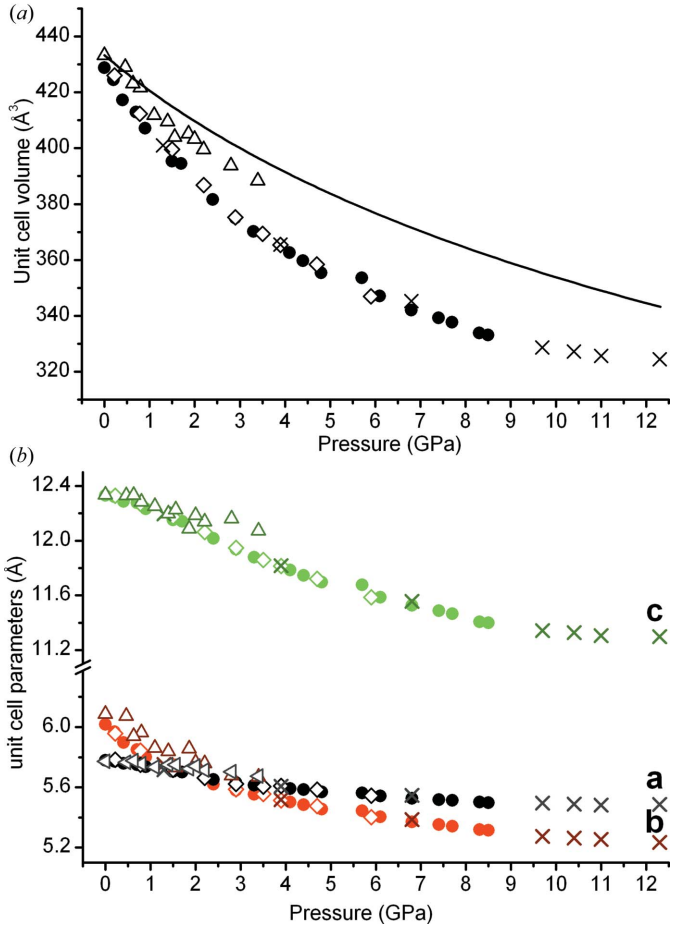

Figure 1
(*a*) The unit-cell volume and (*b*) parameters of L-alanine *versus* pressure (**a**: black, **b**: red, **c**: green). Open circles – the first series of powder experiments, crosses – the second series, rhombs – a single-crystal experiment, triangles – data from Olsen *et al.* (2006, 2008). Solid line – $V(P)$ calculated from Birch–Murnaghan's equation-of-state with the values of coefficients from Olsen *et al.* (2006, 2008). This figure is in colour in the electronic version of this paper.

crystal experiments. Refined cell parameters from powder experiments are summarized in Tables 2, 3 and 4. The structural models have been deposited in the CIF file.[2] The programs *Mercury* (Macrae *et al.*, 2006) and *PLATON* (Spek, 2003) were used for visualization and analysis. Hirshfeld surfaces were calculated using *CrystalExplorer* (McKinnon *et al.*, 2004, 2007; Wolff *et al.*, 2007).

Raman spectra on increasing pressure and reverse decompression were measured in the backscattering geometry using a Horiba Jobin Yvon Lab-Ram HR spectrometer equipped with a N_2 cooled CCD-2048 × 512 detector coupled to an Olympus BX41 microscope. Excitation was supplied by an argon ion laser (λ = 488 nm) with a spectral resolution of 4 cm^{-1}. The same Almax–Boehler DAC, with type II diamonds, was used for the single-crystal diffraction and Raman experiments.

[2] Supplementary data for this paper are available from the IUCr electronic archives (Reference: GP5038). Services for accessing these data are described at the back of the journal.

Table 2
Experimental details, cell parameters and volume from powder diffraction data (first series of experiments).

DAC – Ahsbahs (first series); gasket – hardened Thyrodur-2709, initial thickness – 0.180 mm, after preindentation – 0.104 mm, sample–detector distance 340 mm.

No.	Pressure (GPa)	Time (s)	*a* (Å)	*b* (Å)	*c* (Å)	*V* (Å^3)
1	0†	600	6.018 (5)	5.778 (3)	12.330 (7)	428.8 (3)
2	0.2	1200	5.969 (2)	5.772 (1)	12.321 (2)	424.5 (1)
3	0.4	600	5.896 (2)	5.759 (2)	12.287 (4)	417.2 (1)
4	0.7†	600	5.850 (3)	5.750 (2)	12.276 (5)	412.9 (2)
5	0.9	600	5.802 (4)	5.736 (2)	12.233 (7)	407.1 (3)
6	1.5	600	5.705 (1)	5.705 (1)	12.150 (4)	395.4 (1)
7	1.7†	600	5.700 (1)	5.700 (1)	12.141 (5)	394.5 (1)
8	2.4	600	5.621 (3)	5.651 (2)	12.015 (7)	381.7 (2)
9	2.9	600	5.579 (3)	5.6315 (2)	11.938 (7)	375.0 (2)
10	3.3	600	5.553 (3)	5.613 (1)	11.879 (3)	370.2 (1)
11	4.1	600	5.502 (2)	5.592 (2)	11.786 (3)	362.6 (1)
12	4.4	600	5.485 (2)	5.584 (1)	11.745 (3)	359.7 (1)
13	4.8	600	5.456 (1)	5.568 (1)	11.697 (3)	355.4 (1)
14	5.7†	600	5.443 (3)	5.562 (2)	11.678 (4)	353.6 (2)
15	6.1	600	5.404 (2)	5.543 (2)	11.587 (4)	347.1 (1)
16	6.8	600	5.370 (2)	5.526 (2)	11.527 (3)	342.0 (1)
17	7.4	600	5.352 (2)	5.518 (1)	11.489 (3)	339.3 (1)
18	7.7	600	5.342 (2)	5.514 (2)	11.465 (4)	337.7 (1)
19	8.3	600	5.318 (2)	5.503 (2)	11.408 (4)	333.8 (2)
20	8.5	600	5.315 (2)	5.498 (2)	11.399 (5)	333.1 (2)

† Diffraction patterns are measured on decompression.

Table 3
Experimental details, cell parameters and volume from powder diffraction data (second series of experiments).

DAC – ETH (second series); gasket – stainless steel (ESRF), initial thickness – 0.2 mm, after preindentation – 0.055 mm, sample–detector distance 350 mm.

No.	Pressure (GPa)	Time (s)	*a* (Å)	*b* (Å)	*c* (Å)	*V* (Å^3)
1	1.3	600	5.752 (3)	5.717 (1)	12.195 (5)	401.0 (2)
2	3.9	600	5.517 (2)	5.606 (1)	11.818 (3)	365.5 (1)
3	6.1	600	5.386 (1)	5.548 (8)	11.556 (2)	345.26 (7)
4	9.7	7200	5.273 (2)	5.495 (1)	11.342 (2)	328.62 (9)
5	10.4	3600	5.264 (2)	5.488 (1)	11.328 (2)	327.3 (1)
6	11.0	3600	5.254 (3)	5.482 (2)	11.306 (3)	325.6 (2)
7	12.3	600	5.233 (8)	5.487 (4)	11.300 (7)	324.5 (5)

3. Results and discussion

3.1. Continuous structural changes induced by increasing pressure

The changes in unit-cell parameters and volume of L-alanine *versus* pressure are plotted in Fig. 1. The data in the two series of our X-ray diffraction synchrotron powder experiments agree with each other, as well as with the single-crystal diffraction experiments using a laboratory diffractometer, but deviate noticeably from the absolute values reported in Olsen *et al.* (2006, 2008). Neither of the two structural phase transitions (at 2.3 and at 9 GPa) reported in Olsen *et al.* (2006, 2008) were observed in our experiments. The curves $a(P)$ and $b(P)$ cross each other at ~ 2 GPa, so the two parameters become accidentally equal in this pressure range. The powder pattern at this pressure could be indexed formally in a tetragonal cell, but the subsequent continuous

Table 4
Experimental details, cell parameters and volume from powder diffraction data (third series of experiments).

Boehler–Almax DAC (identifying of the polycrystalline phases); gasket – Inconel 718, initial thickness – 0.25 mm, after preindentation – 0.09 mm, sample–detector distance 302 mm.

No.	Pressure (GPa)	Time (s)	*a* (Å)	*b* (Å)	*c* (Å)	*V* (Å^3)	Phase
1	0	600	5.780 (1)	6.049 (2)	12.345 (3)	431.6 (1)	L-Alanine
2	0.3	600	5.774 (2)	5.960 (2)	12.337 (4)	424.6 (2)	L-Alanine
3	0.4	1200	5.759 (2)	5.929 (4)	12.321 (6)	420.7 (3)	L-Alanine
4	0.8	1200	4.6856 (7)	8.699 (2)	10.019 (2)	408.4 (1)	Second 'solvate'
5	1.1	1200	4.668 (1)	8.567 (2)	10.012 (3)	400.4 (2)	Second 'solvate'
6	1.4	1200	4.697 (4)	8.436 (5)	16.259 (2)	644.2 (7)	First 'solvate'
7	1.6	1200	4.6852 (7)	8.387 (1)	16.224 (3)	637.6 (2)	First 'solvate'
8	1.9	1200	4.6725 (8)	8.337 (1)	16.174 (3)	630.0 (2)	First 'solvate'
9	2.2	1200	4.658 (1)	8.274 (2)	16.114 (3)	621.1 (2)	First 'solvate'
10	2.6	1200	4.6428 (7)	8.210 (2)	16.059 (3)	612.2 (1)	First 'solvate'
11	2.9	1200	4.637 (1)	8.179 (2)	16.043 (3)	608.4 (2)	first 'solvate'
12	3.4	600	4.6218 (1)	8.115 (1)	15.994 (3)	599.9 (1)	First 'solvate'
13	3.8	1800	4.608 (1)	8.069 (1)	15.938 (3)	592.6 (1)	First 'solvate'

The measurements were carried out on decompression from 3.8 GPa down to ambient pressure.

changes in the cell parameters at higher pressures suggest that the symmetry remains orthorhombic. In fact, attempts to solve the structure in a tetragonal group based on the powder diffraction data at this pressure failed, whereas the structure solution and refinement in the original orthorhombic $P2_12_12_1$ group were successful. Single-crystal experiments in the pressure range up to 5.9 GPa at nine different pressure points have proved unambiguously that the orthorhombic space-symmetry group was preserved at least in this pressure range. For the higher pressure range, where only powder-diffraction data were available, structure solution and refinement was also possible only in the original orthorhombic space-symmetry group, and there was no indication of a possible monoclinic distortion of the structure (see Tables 2 and 3).[3]

Although the high-pressure data even from single-crystal diffraction experiments have a lower precision than the low-temperature data collected for 'free crystals', the main trends in changes in intermolecular contacts and even in selected intramolecular bond lengths could be followed. The same trends (but of course not the same absolute values) were observed, independent of whether powder or single-crystal diffraction data were used, and, for single-crystal diffraction data, whether an isotropic or anisotropic refinement or a TLS correction was made or not. This allows us to conclude that the trends are real and not artifacts.

All the intermolecular distances in the crystal structure of L-alanine changed continuously with increasing pressure. Since the CH_3 groups in L-alanine are not involved in the formation of strong hydrogen bonds (in contrast to what holds for the CH_2OH groups in serine), no rotation of the side chains took place with increasing pressure, the amino acid zwitterion preserved its conformation, and no structural phase transitions occurred. The intermolecular contacts of interest for further discussion are shown in Figs. 2 and 3. Single-crystal diffraction data, as the most precise and accurate, have been used to analyze the changes in intramolecular geometry (Table 5) and these contacts (Table 6) in detail (Fig. 4).

The main effects of increasing pressure on the crystal structure of L-alanine can be summarized as follows: the N—

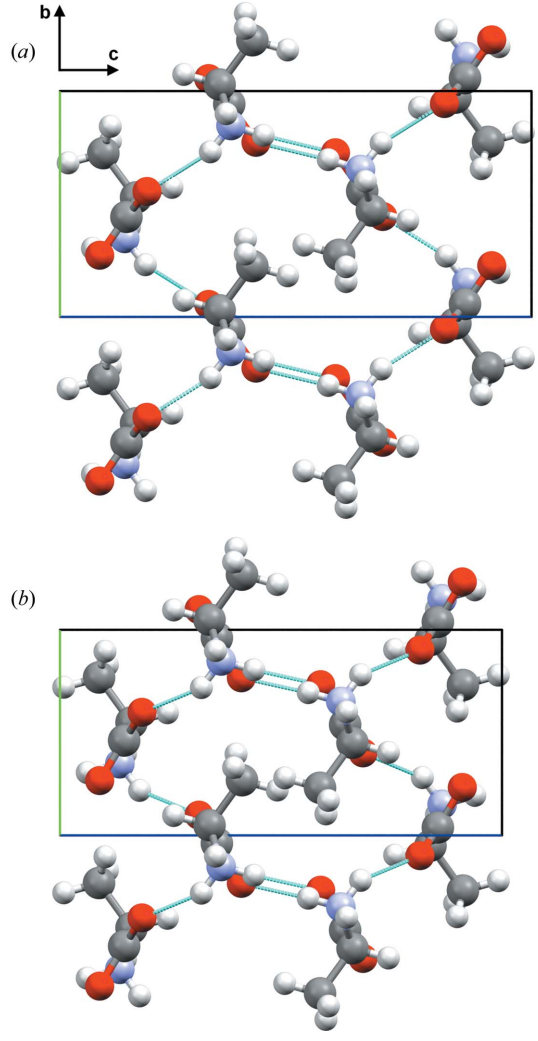

Figure 2
Fragments of the L-alanine structure at (*a*) 0.2 GPa and (*b*) 5.9 GPa. No structural phase transition occurs. This figure is in colour in the electronic version of this paper.

[3] In a recent review by Moggach *et al.* (2008) it was briefly mentioned that the authors of the review also have some unpublished data on the single-crystal diffraction of L-alanine that 'appear to indicate that the space-group symmetry $P2_12_12_1$ is preserved at least until 7.2 GPa and the crystal structure at 2.3 GPa is only metrically tetragonal', but no data were published. By the time this paper was in proof, the data became available on the Web (Funnell *et al.*, DOI: 10.1039/c001296c, submitted 20 January 2010), also confirming the absence of phase transitions with a space-group symmetry change in L-alanine at pressures up to 8.1 (X-ray single-crystal diffraction) and 9.87 GPa (neutron powder diffraction).

H···O hydrogen bonds, C—H···O contacts and the C—C distances in the CH_3—CH_3 contacts became shorter. The shortening of all the intermolecular contacts slowed down with pressure, but no special features have been observed in the supposed phase transition region. Hirshfeld fingerprints plots and surfaces (Figs. 5 and 6) give a general picture of what happens to the short contacts in the crystal structure with increasing pressure. There is relatively little change in the short H—H and O—H contacts, but a much more important reduction of the longer contacts in the structure upon compression.

Relative compression of the three different types of N—H···O hydrogen bonds was different, so the shortest N—H···O hydrogen bond in the crystal structure at ambient pressure, namely that linking L-alanine zwitterions within a head-to-tail chain (N1—H12···O1), became the longest one at ~ 2–3 GPa (Fig. 4).

Some changes could be followed for selected intramolecular bond lengths and angles. Interestingly, at ambient conditions, in contrast to some crystalline amino acids, the two C—O bonds in the COO group are not absolutely equal in L-alanine. This was also confirmed by several independent X-ray and

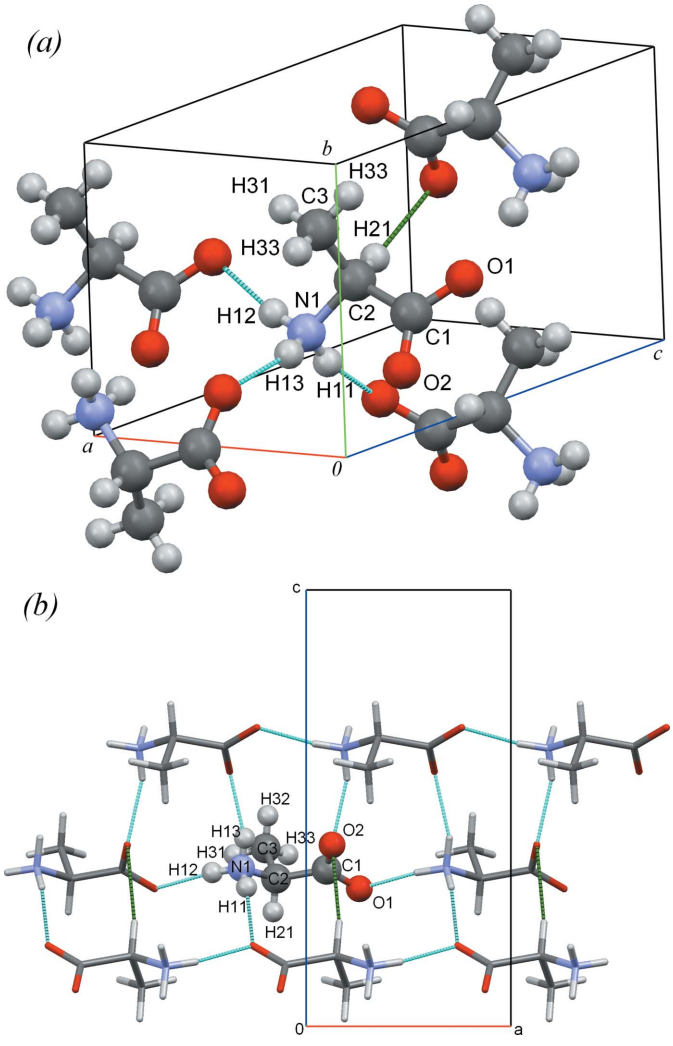

Figure 3
N—H···O hydrogen bonds (blue dashed lines) and short C—H···O contacts (green dashed lines) in L-alanine at 0.2 GPa. (*a*) This orientation illustrates that the different relative compressibility values of the three types of N—H···O hydrogen bonds are closely interrelated with the orientation of the NH_3^+ tail and its torsion motions. (*b*) Head-to-tail chains of zwitterions and the difference in types of N—H···O hydrogen bonds formed by the two different O atoms are seen more clearly in this orientation. The numbering of atoms is shown. This figure is in colour in the electronic version of this paper.

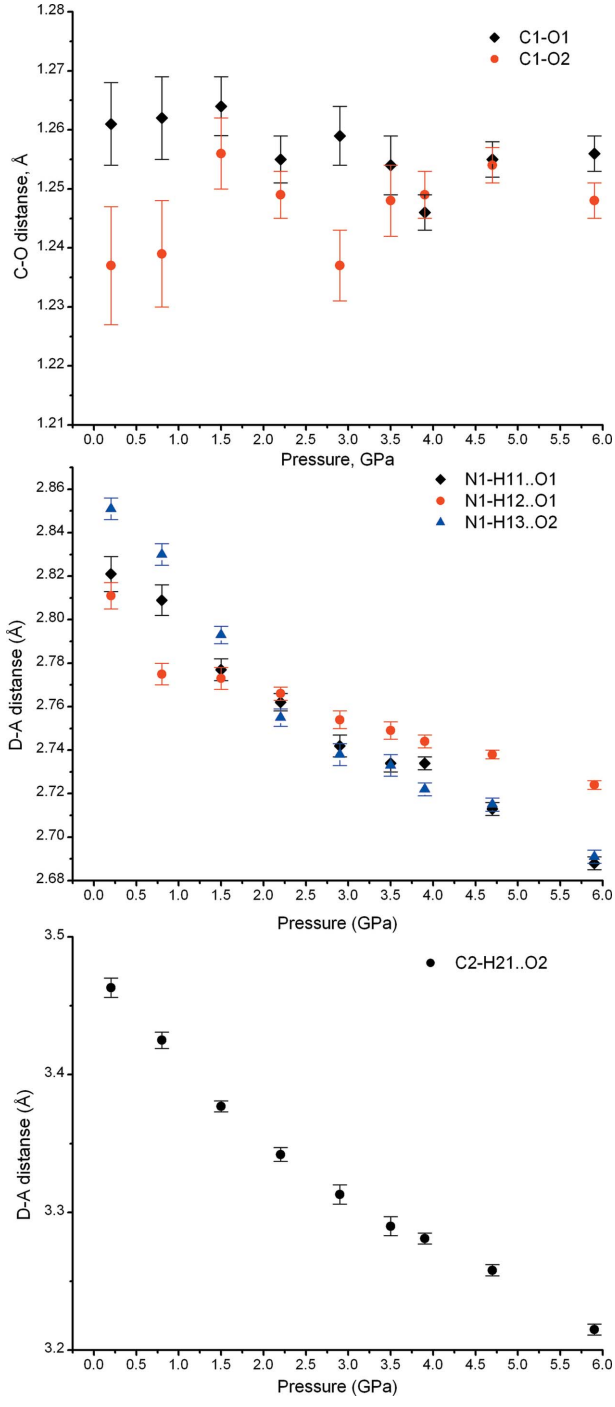

Figure 4
(*a*) Intramolecular C—O distances, (*b*) intermolecular N—O distances in the NH···O hydrogen bonds, and (*c*) C—O distances in the CH···O contacts *versus* pressure.

Table 5
Selected intramolecular geometric parameters (Å, °) at different pressures.

The numbering of the atoms is shown in Fig. 3.

	0.2 GPa	0.8 GPa	1.5 GPa	2.2 GPa	2.9 GPa
C1—O1	1.261 (7)	1.262 (7)	1.264 (5)	1.255 (4)	1.259 (5)
C1—O2	1.237 (10)	1.239 (9)	1.256 (6)	1.249 (4)	1.237 (6)
C2—C1	1.538 (7)	1.540 (7)	1.529 (5)	1.531 (4)	1.533 (5)
C2—C3	1.477 (14)	1.465 (12)	1.506 (7)	1.514 (4)	1.494 (6)
C2—N1	1.490 (11)	1.483 (10)	1.504 (6)	1.488 (4)	1.471 (6)
C3—C2—N1	108.7 (4)	109.6 (4)	110.1 (3)	109.3 (3)	110.2 (4)
C3—C2—C1	110.8 (5)	111.9 (4)	108.4 (4)	109.3 (3)	108.8 (4)
N1—C2—C1	109.9 (8)	109.0 (7)	111.7 (3)	111.7 (3)	111.8 (3)
O2—C1—O1	125.6 (4)	125.5 (4)	125.4 (3)	126.2 (3)	125.8 (3)
O2—C1—C2	118.6 (6)	119.2 (5)	119.3 (3)	118.2 (3)	118.8 (4)
O1—C1—C2	115.8 (7)	115.3 (7)	115.3 (4)	115.6 (3)	115.3 (4)
C3—C2—C1—O1	−78.0 (6)	−76.5 (6)	−74.8 (4)	−73.7 (6)	−72.5 (7)
C3—C2—C1—O2	101.8 (10)	102.3 (9)	104.1 (5)	104.6 (5)	105.3 (6)
N1—C2—C1—O1	161.8 (5)	162.2 (4)	163.7 (3)	165.2 (3)	165.5 (4)
N1—C2—C1—O2	−18.4 (8)	−19.0 (7)	−17.4 (5)	−16.5 (6)	−16.6 (7)

	3.5 GPa	3.9 GPa	4.7 GPa	5.9 GPa
C1—O1	1.254 (5)	1.246 (3)	1.255 (3)	1.256 (3)
C1—O2	1.248 (6)	1.249 (4)	1.254 (3)	1.248 (3)
C2—C1	1.526 (5)	1.536 (3)	1.521 (3)	1.517 (3)
C2—C3	1.497 (6)	1.496 (4)	1.487 (4)	1.489 (4)
C2—N1	1.468 (5)	1.464 (4)	1.460 (4)	1.459 (3)
C3—C2—N1	110.5 (4)	110.1 (3)	110.0 (2)	109.8 (2)
C3—C2—C1	109.4 (4)	109.3 (2)	110.0 (2)	109.6 (2)
N1—C2—C1	112.3 (4)	111.6 (3)	112.4 (3)	111.8 (2)
O2—C1—O1	125.6 (3)	125.4 (2)	125.1 (2)	125.1 (2)
O2—C1—C2	118.2 (4)	116.2 (2)	118.2 (2)	118.7 (2)
O1—C1—C2	116.1 (4)	118.3 (3)	116.6 (2)	116.1 (2)
C3—C2—C1—O1	−70.9 (7)	−72.6 (5)	−70.2 (5)	−71.2 (4)
C3—C2—C1—O2	106.6 (6)	165.4 (3)	105.8 (4)	106.4 (4)
N1—C2—C1—O1	166.0 (4)	105.8 (4)	166.9 (3)	166.9 (2)
N1—C2—C1—O2	−16.5 (8)	−16.2 (5)	−17.1 (5)	−15.6 (5)

Table 6
Geometric parameters (Å, °) for hydrogen bonds and short intermolecular contacts at different pressures.

D—H···A	D—H (Å)	H···A (Å)	D···A (Å)	D—H···A (°)
0.2 GPa				
N1—H11···O1^{i}	0.89	1.97	2.821 (8)	160.0
N1—H12···O1^{ii}	0.89	1.93	2.811 (6)	169.6
N1—H13···O2^{iii}	0.89	1.99	2.851 (5)	161.4
0.8 GPa				
N1—H11···O1^{i}	0.89	1.96	2.809 (7)	159.5
N1—H12···O1^{ii}	0.89	1.90	2.775 (5)	169.1
N1—H13···O2^{iii}	0.89	1.97	2.830 (5)	162.3
1.5 GPa				
N1—H11···O1^{i}	0.89	1.92	2.777 (5)	160.3
N1—H12···O1^{ii}	0.89	1.91	2.773 (4)	164.1
N1—H13···O2^{iii}	0.89	1.95	2.793 (4)	157.8
2.2 GPa				
N1—H11···O1^{i}	0.89	1.94	2.762 (4)	153.8
N1—H12···O1^{ii}	0.89	1.90	2.766 (3)	165.5
N1—H13···O2^{iii}	0.89	1.89	2.755 (4)	162.2
2.9 GPa				
N1—H11···O1^{i}	0.89	1.94	2.742 (5)	149.0
N1—H12···O1^{ii}	0.89	1.89	2.754 (4)	163.4
N1—H13···O2^{iii}	0.89	1.87	2.738 (5)	166.1
3.5 GPa				
N1—H11···O1^{i}	0.89	1.93	2.734 (4)	148.9
N1—H12···O1^{ii}	0.89	1.89	2.749 (4)	162.8
N1—H13···O2^{iii}	0.89	1.86	2.733 (5)	166.6
3.9 GPa				
N1—H11···O1^{i}	0.89	1.92	2.734 (3)	152.2
N1—H12···O1^{ii}	0.89	1.88	2.744 (3)	162.6
N1—H13···O2^{iii}	0.89	1.87	2.722 (3)	159.9
4.7 GPa				
N1—H11···O1^{i}	0.89	1.92	2.713 (3)	148.1
N1—H12···O1^{ii}	0.89	1.88	2.738 (2)	162.4
N1—H13···O2^{iii}	0.89	1.84	2.715 (3)	166.3
5.9 GPa				
N1—H11···O1^{i}	0.89	1.90	2.688 (3)	147.3
N1—H12···O1^{ii}	0.89	1.87	2.724 (2)	161.4
N1—H13···O2^{iii}	0.89	1.82	2.691 (3)	164.3

Symmetry codes: (i) $-x, y-\frac{1}{2}, -z+\frac{1}{2}$; (ii) $x+1, y, z$; (iii) $x+\frac{1}{2}, -y+\frac{1}{2}, -z$.

neutron diffraction studies, also after a TLS correction (Barthes *et al.*, 2004; Destro *et al.*, 1988, 1991, 2008; Dunitz & Ryan, 1966; Lehmann *et al.*, 1972; Wilson *et al.*, 2005). In our experiments in a DAC, the two C—O bonds were not equivalent at ambient pressure, the difference being of the order of that observed by other authors, *e.g.* Destro and co-workers. The difference in length of these two intramolecular C—O bonds in the carboxylic group decreased with pressure. The compression of the two hydrogen bonds (N1—H11···O1 and N1—H12···O1) was accompanied by shortening of the longer C—O1 bond, whereas the shortening of the hydrogen bond N1—H13···O2 resulted in the elongation of the shorter C—O2 bond (in agreement with the Raman spectra, see below).

The pressure-induced changes in the intra- and intermolecular distances in the crystal of L-alanine agree very well with the general properties of the N—H···O hydrogen-bond linking zwitterions within a chain, further defined as N*—H*···O* to distinguish it from other N—H···O bonds in the structure (Kolesov & Boldyreva, 2010*a*,*b*). The formation of zwitterions rather than neutral molecules in the crystals of amino acids is related to the formation of a hydrogen bond between the NH_3^+ and the COO^- groups after a proton moves from the COOH group of one amino acid molecule in a chain to the NH_2 group of another molecule; L-alanine is no exception. For glycine, sarcosine and *N*,*N*-dimethylglycine, the shift of the proton resulting in the formation of zwitterions from neutral molecules was observed directly in the solid state, and other intermolecular interactions in the solid phase were supposed to play an important role in the mechanism of proton transfer (Gómez-Zavaglia & Fausto, 2003). The mechanism for its formation makes the properties of the N*—H*···O* bond unusual compared with other 'ordinary' N—H···O hydrogen bonds, which are not related to proton transfer from one species to another by their origin. When an 'ordinary' N—H···O hydrogen bond expands (the distance between a donor N and an acceptor O increases), the proton

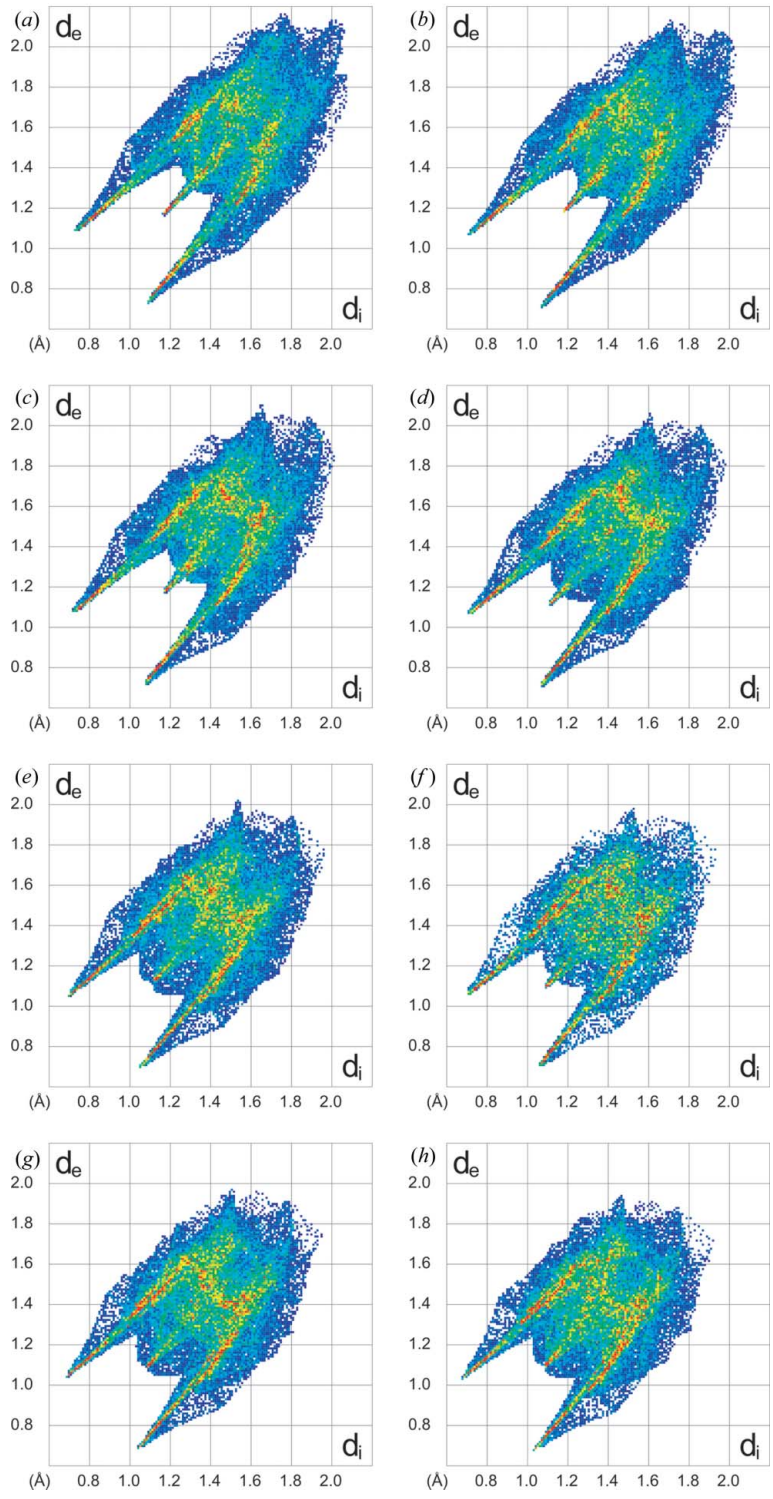

Figure 5
Two-dimensional Hirshfeld fingerprint plots of L-alanine structure at (*a*) 0.2 GPa, (*b*) 0.8 GPa, (*c*) 1.5 GPa, (*d*) 2.2 GPa, (*e*) 3.5 GPa, (*f*) 3.9 GPa, (*g*) 4.7 GPa and (*h*) 5.9 GPa. The colour in the sequence white–blue–green–red is a summary of the frequency of each combination of distances d_e and d_i across the surface of a molecule (in increasing order), where d_i is internal distance and d_e external distance from the Hirshfeld surface to the nearest molecule. The features along the diagonal occur due to H—H contacts, while the 'wings' are due to O—H and C—H interactions. See more details in Fig. 12.

shifts in the direction of the donor atom so that the N—H distance decreases and the wavenumber of the NH stretching vibration increases. This does not hold, however, for a N*—H*···O* bond. In a hypothetical extreme situation, when the distance between the molecules in a chain is large enough to exclude the interaction between the alanine molecules in a chain, the H* atom would be back at the carboxylic group and the molecules would no longer be zwitterionic, *i.e.* on extreme extension of a N*—H*···O* bond the proton would move from N* to O*. Compressing or expanding the structure can favor a shift of the H* atom along the N*—H*···O* bond. This proton shift in L-alanine or some other amino acids could be induced by temperature variations, either cooling well below ambient temperature (Kolesov & Boldyreva, 2010*a*,*b*) or heating close to the melting temperatures (Peterson & Nash, 1985), and could manifest itself, for example, in the Raman or FTIR spectra. At high temperatures (close to the melting point) the interaction between the molecules weakens and the proton shifts towards oxygen, its 'original donor'. This was reported for crystalline *N*,*N*-dialkylated amino acids by Peterson & Nash (1985). When the chain of zwitterions is compressed and the distance between the molecules shortens, the opposite effect is expected: the interaction between the carboxylic group and the amino group becomes stronger, and the proton shifts further towards the amino group so that the polarization of the zwitterions increases. This effect accounts for a variety of anomalies observed in the crystalline L-alanine on cooling down to 3 K (Kolesov & Boldyreva, 2010*a*,*b*). A similar but much stronger effect (a practically complete transfer of a proton between two neutral molecules to give ions, not just a small shift along a hydrogen bond linking two zwitterions) has been observed on cooling for the urea–phosphoric acid (1:1) complex (Wilson, 2001), for the 1:1 squaric acid-4,4′-bipyridine adduct (Martins *et al.*, 2009), and also at high pressure for the oxalic acid dihydrate (Casati *et al.*, 2009; Casati, 2010).

The longer of the two non-equal C—O bonds in the crystalline L-alanine is that which is involved in the formation of the N*—H*···O* bond in the head-to-tail chain of zwitterions. This difference may suggest that the proton transfer from the COOH head of one L-alanine molecule to the NH_2 tail of

another L-alanine molecule, which results in the formation of zwitterions, is not absolutely complete at any temperature at ambient pressure. The non-equality in the C—O bond lengths in the carboxylic group may serve as a measure of the completeness of the H*-atom transfer between two alanine zwitterions within a chain. An alternative interpretation of the different lengths of the two C—O bonds in L-alanine is that this difference reflects the difference in the total number of hydrogen bonds formed by two different O atoms. In fact, this is the explanation which has been proposed in previous publications. This simple explanation may be, of course, true. However, it does not explain why in crystalline glycine (where the two O atoms of a carboxylic group are also involved in the formation of a different number of intermolecular hydrogen bonds) the two C—O bonds are equal in length (Jönsson & Kvick, 1972). The difference in the number of hydrogen bonds in which the two O atoms are involved cannot explain why the difference in bond length becomes noticeably smaller with increasing pressure (the number of hydrogen bonds formed by each atom is still different at higher pressures), and why the compression of the two hydrogen bonds (N1—H11···O1 and N1—H12···O1) is accompanied by anomalous shortening of the C—O1 distance, as if the interaction between O with H was weakened. However, shortening of the hydrogen bond N1—H13···O2 results in the elongation of the C—O2 distance, as expected for a 'normal' hydrogen bond, in which the interaction between O and H becomes stronger. Moreover, in the pressure range above 2–3 GPa, when the lengths of the C—O bonds are similar and are similar to the value reported for glycine, the N—O distance in the N*—H*···O* bond also becomes similar to that in glycine at ambient pressure (Jönsson & Kvick, 1972). It looks as if in L-alanine at ambient pressure the more bulky $-C(H)-CH_3$ groups (compared with the $-CH_2$ groups in glycine) prevent the molecules in the head-to-tail chains from approaching each other at a distance which would be short enough to 'complete' the proton transfer between the zwitterions to such an extent that the two C—O bonds in a carboxylic group become equal.

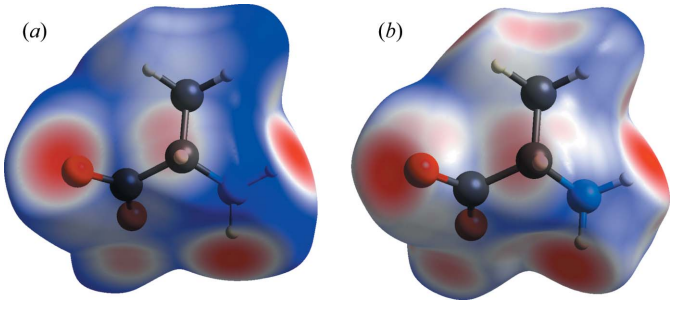

Figure 6
Hirshfield surface at (*a*) 0.2 GPa and (*b*) 5.9 GPa. Blue areas (long contacts) quickly shortened on compression. The plot represents the normalized contact distances in the range from −0.68 to 0.8 Å, where the normalization is by the van der Waals radii of the atoms involved. The white regions represent contacts around the sum of the van der Waals radii, the red spots represent intermolecular contacts closer than the sum of their van der Waals radii, whereas longer contacts are shown in blue.

Increasing the pressure makes it possible to bring the carboxylic and the amino groups of neighboring zwitterions in a chain closer to each other, to the distance at which in glycine they are already at ambient pressure, and the C—O bonds become more equivalent. We realise that this is a model, a suggestion, but this model is based on experimental findings. Although the quality of high-pressure structure refinement is surely limited compared with the low-temperature data measured for 'free crystals', and we cannot follow the positions of the H atoms directly, the data on the coordinates of non-H atoms are reliable enough to measure the changes in distances between the non-H atoms, which provides indirect evidence on the changes in hydrogen positions. Besides, the changes in the hydrogen bonds manifest themselves in the Raman spectra: we cannot follow the variations in the N—H stretching vibration wavenumbers in the high-pressure spectra (too weak bands), but we do see the changes in the two C—O stretching vibrations with increasing pressure (quite unusual in that the wavenumber of the symmetric mode increases while that of the asymmetric vibration changes very little; in the case of weak dynamic interactions between two C—O

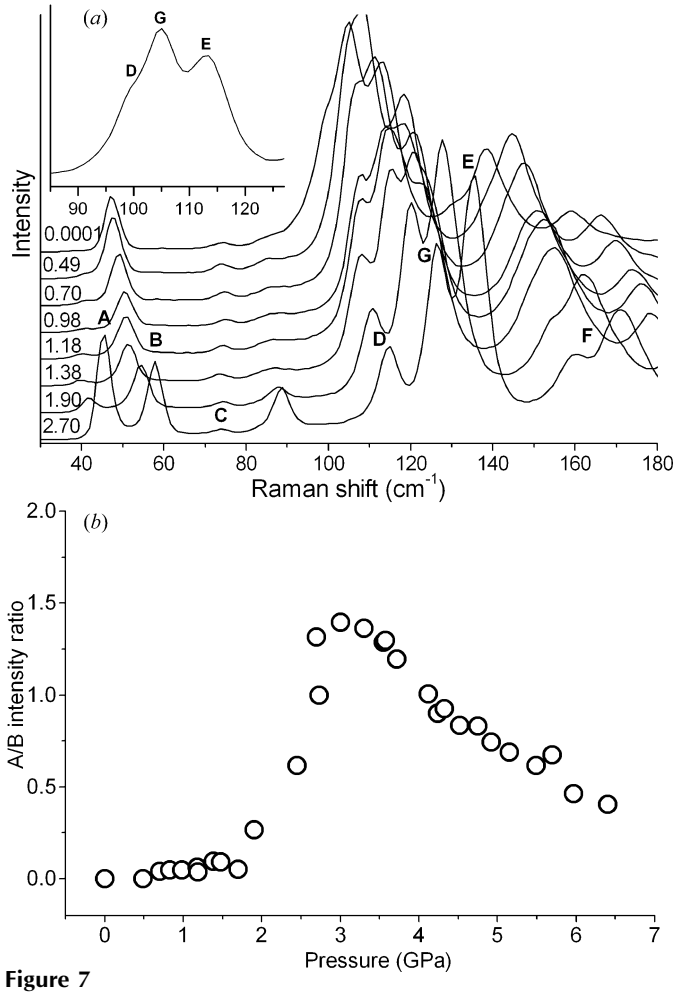

Figure 7
(*a*) Raman spectra of L-alanine in the range of low wavenumbers at different pressures. The numbers indicate the pressure values in GPa. Inset: magnified part of the spectrum in the range 90–120 cm^{-1} at ambient pressure. (*b*) The ratio of the intensities of *A* and *B* peaks *versus* pressure.

bonds this means an opposite change in the force constants of these two bonds). Significant changes can then be seen in the lattice modes in the same pressure range, where the C—O bond lengths become closer to each other.

Changes in the range of lattice modes in the Raman spectra of crystalline L-alanine[4] at ~ 2–3 GPa, namely a sharp redistribution in the intensities of the two vibrational bands at 42 and 49 cm^{-1} (maxima positions at ambient conditions), termed *A* and *B* in the original publication, and an emergence of a new vibrational band termed *G* at ~ 110 cm^{-1}, served as the main arguments in favor of a structural phase transition with a symmetry change (Olsen *et al.*, 2008). In our experiments, performed over a somewhat wider pressure range, the change in intensity ratio of *A* and *B* bands was similar to that reported by Teixeira *et al.* (2000), but the amplitude of the effect differed. This could be a consequence of the different crystal orientations in the two experiments (Fig. 7). A higher resolution version of our spectra made it possible to see that the *G* band is present in the Raman spectrum at ambient pressure, and that on increasing the pressure the group of vibrational *D*, *E* and *G* bands splits and all three peaks become very well resolved. The *F* band also consists of two peaks which split as pressure increases. In addition, one more peak between the *C* and *D* peaks at ~ 85 cm^{-1} (at ambient pressure) is present in the Raman spectra, which has not been described in previous publications (Teixeira *et al.*, 2000; Olsen *et al.*, 2006, 2008), and its intensity increases noticeably on compression. Thus, in general, our Raman data agree with the spectra measured by Teixeira *et al.* (2000), but all the changes are continuous and no new bands appear. Thus, the spectral changes are not related to any structural polymorphic transformations with a space-group symmetry change, but are typical for changes in the dynamics of the intermolecular hydrogen bonds (related to proton shifts along hydrogen bonds, different compression of different types of hydrogen bonds, rotations of selected hydrogen-bonded fragments, changes in their torsion barriers *etc.*). The changes in the hydrogen-bond networks are often induced by variations in temperature and pressure. They can be responsible for structural phase transitions or, as in the case of L-alanine, can be related to a continuous structural distortion and dynamic effects (Katrusiak, 1990, 1991, 1992, 1993, 1995, 1996, 2001, 2004, 2010).

3.2. Reversible crystallization of new polycrystalline phases at high pressure

While studying the reversible and continuous pressure-induced structural distortion in single crystals of L-alanine by single-crystal X-ray diffraction using a laboratory X-ray source and hence collecting data at each point for several days, we observed a phenomenon which, to the best of our knowledge, has never been reported before for L-alanine: crystallization of a new polycrystalline phase in the 0.8–4.7 GPa pressure range co-existing with the starting single crystal of L-alanine, which converted back to L-alanine on reverse decompression.

In the first series of single-crystal diffraction experiments, when pressure was increased very slowly from ambient upwards and kept at intermediate values for 1–2 d, the dimensions of the L-alanine crystal changed with increasing pressure (Fig. 8). At 2.2 GPa the visible crystal size (0.14 × 0.05 mm) was approximately half the initial size. At 3.7 GPa, 6 h after the start of the experiment, part of the crystal recrystallized into a polycrystalline sample (see Fig. 8*h*), and the pressure decreased to 3.5 GPa on its own. On reverse decompression, at ~ 2.1 GPa, we observed a recrystallization of the polycrystalline sample into the single crystal so that the crystal was restored to its original size. A single-crystal X-ray diffraction experiment was carried out at this pressure. We observed a strange crystal-size oscillation during this experiment (see Figs. 8*i*, *j* and *k*). Immediately after the data collection the visible size of the crystal was smaller than

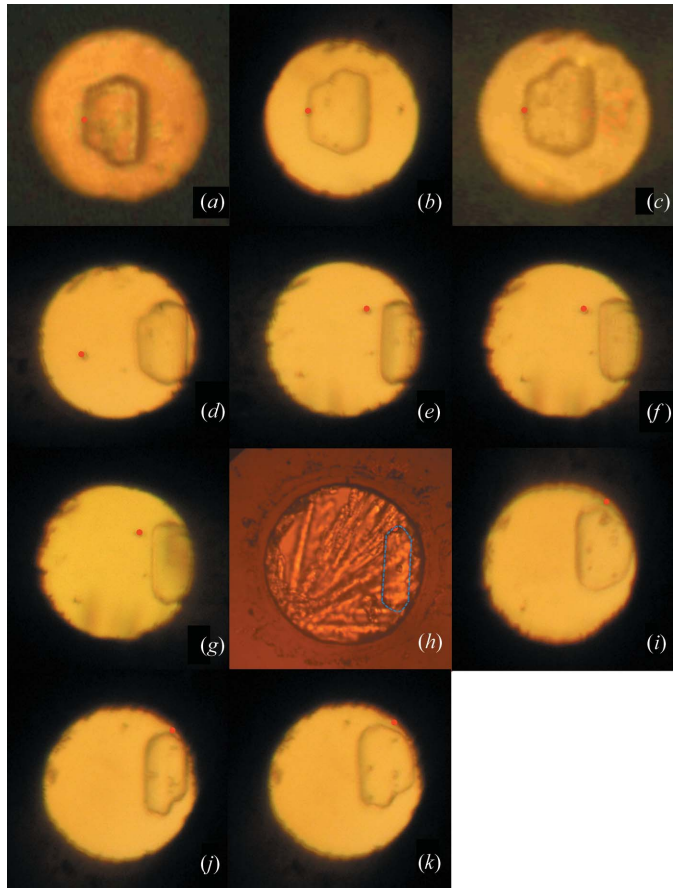

Figure 8
Photographs of the L-alanine crystal in the diamond–anvil cell at (*a*) 0.2 GPa, (*b*) 0.8 GPa, 1.5 GPa (*c*) before and (*d*) after an X-ray diffraction experiment, (*e*) 2.2 GPa, (*f*) 2.9 GPa, (*g*) 3.7 GPa (before experiment) and (*h*) 3.5 GPa (after experiment), (*i*) 2.1 GPa (decompression) before, (*j*) after experiment and (*k*) 10 min later. Red point – position of the ruby sphere. The blue dashed line at (*h*) marks the position of the crystal, which becomes poorly seen after partial recrystallization. Insert shows the 90–120 cm^{-1} range of the spectrum measured at ambient pressure.

[4] The bands in the 40–150 cm^{-1} range were assigned as lattice vibrations. The intensive A and B modes at 115–130 cm^{-1} can be assigned rather definitely to lattice translations (Kolesov & Boldyreva, 2010*b*).

the initial one at ~ 30%, but 10 min later the initial size of the crystal was restored. The exact reasons for this unusual recrystallization and the visible changes.[5] in the crystal size remain unclear. Temperature variation in the 273–323 K range did not lead to any pronounced changes in the crystal size or dissolution behavior. Additional comparative experiments with L-alanine crystals in methanol–ethanol (4:1) and methanol–ethanol–water (16:3:1) media, when the single crystal was compressed and simultaneously observed through an optical microscope, have shown that the presence of water in the pressure-transmitting liquid had no noticeable effect on the phenomenon described. The crystallization of the new polycrystalline phase was observed only when the sample was kept at a pressure close to 3.5–4.7 GPa over a long time, which is the case for single-crystal diffraction experiments but not in standard Raman experiments, when pressure was increased quickly and the sample was not kept at each pressure point longer than 1–2 h. The duration of keeping a crystal at a selected pressure is known to influence kinetically controlled transformations quite considerably (Boldyreva, 2007*b*).

To additionally test the role of kinetic factors in the crystallization one more series of experiments was performed, in which a single-crystal of L-alanine was quickly compressed up to 5.9 GPa in a MeOH–EtOH–water (16:3:1) medium. The single-crystal of L-alanine was preserved at this pressure for several months, and no crystallization of a polycrystalline phase was observed. When we started to decompress the sample slowly, collecting diffraction data at pressure points 5.9, 4.7 and 3.9 for 1–2 d, and measuring Raman spectra from the same sample, the crystallization of a new polycrystalline phase started at 4.7 GPa (Fig. 9*b*), which was then followed by optical microscopy, Raman spectroscopy and X-ray diffraction at certain time points. A maximum new phase was obtained at 3.8 GPa. The Raman spectra of the new phase (Fig. 10) suggested that it was a solvate of L-alanine: the bands of the solvent were present in the spectra of the new phase, in addition to the bands of L-alanine, but the position of all the lines was shifted compared with those in pure L-alanine or in pure solvent.[6] The synchrotron powder diffraction patterns measured for the new phase (Fig. 11) could be indexed in the $P2_12_12_1$ space group with unit-cell parameters 4.608 (9), b = 8.0686 (4), c = 15.938 (3) Å, V = 592.6(1) Å^3 (at 3.8 GPa). The sample was further decompressed in small steps (0.3 GPa per 40 minutes) and at ~ 1.4 GPa the sample darkened and the reflections from one more polycrystalline phase appeared in the diffraction pattern. Three phases (a single-crystalline L-alanine and two unknown polycrystalline phases, presumably, 'solvates') co-existed at this pressure. The first 'solvate' was no longer observed at the next pressure point (1.1 GPa). The powder pattern of the second 'solvate' at this pressure could be indexed in the orthorhombic system with the unit-cell parameters a = 4.6683 (12), b = 8.567 (2), c = 10.012 (3) Å, V = 400.38 (14) Å^3. The second 'solvate' was observed on decompression down to 0.4 GPa (see Fig. 9*k*, the remaining crescent-shaped phase is the rest of the second 'solvate') and at the same pressure the reflections of the polycrystalline L-alanine appeared in the diffraction pattern, in addition to the reflections of the unknown phase. At 0.3 GPa only the reflections of L-alanine could be observed in the diffraction

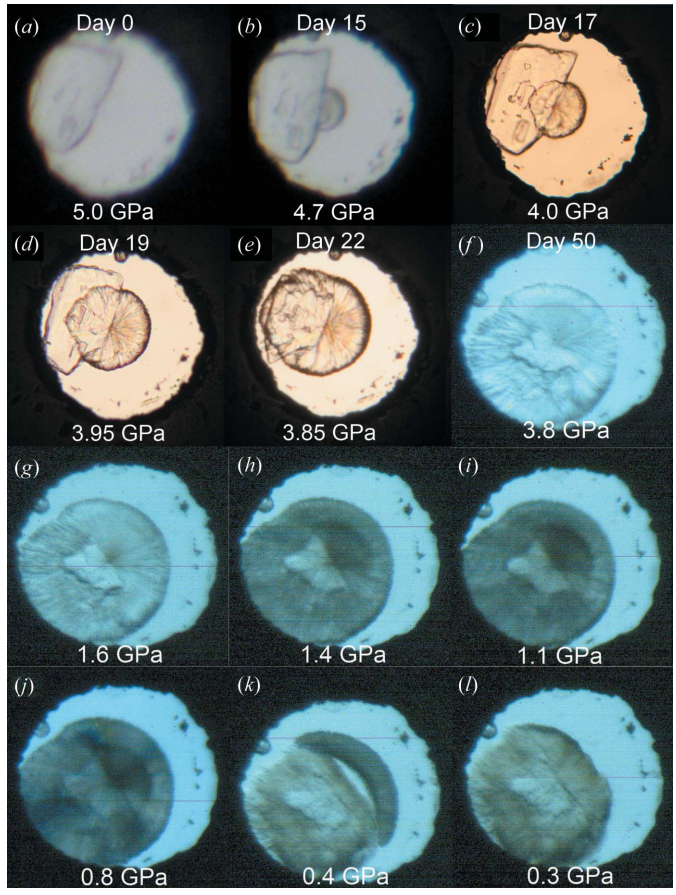

Figure 9
Photographs of the sample (originally a single crystal of L-alanine) in the diamond–anvil cell representing recrystallization into two new polycrystalline phases in the second series of experiments (rapid compression and then slow decompression: [(*a*) 5.0 GPa, (*b*) 4.7 GPa, (*c*) 4.0 GPa, (*d*) 3.95 GPa, (*e*) 3.85 GPa, (*f*) 3.8 GPa, (*g*) 1.6 GPa, (*h*) 1.4 GPa, (*i*) 1.1 GPa, (*j*) 0.8 GPa, (*k*) 0.4 GPa and (*l*) 0.3 GPa]. The single crystal was compressed up to 6 GPa and kept at this pressure for several months without any changes. After that it was decompressed down to 4.7 GPa, when the crystallization of the polycrystalline phase started. The first 'solvate' phase was growing as a 'spherulite' from a nucleation center at the surface of the original L-alanine crystal, which simultaneously decreased in size (*b*,*c*,*d*,*e*,*f*). The sample darkened near 1.4 GPa (*h*) because of a partial transformation into the second 'solvate' phase. The second 'solvate' was observed down to 0.4 GPa – (*k*) the remaining crescent-shaped phase is the rest of the second 'solvate'. All other parts of the sample consisted of single-crystalline and polycrystalline L-alanine. It is indicated directly in photographs (*a*)–(*f*) how long the sample has been kept at a selected pressure after the decompression started. All the photographs after (*f*) were taken during day 50. The pressure decreased from 5.0 GPa down to 4.7 GPa on its own, was then reduced down to 4.0 GPa by an experimentalist and decreased further down to 3.8 GPa on its own; the further decrease in pressure was carried out by an experimentalist.

[5] The thickness of the crystal was not measured, *i.e.* we followed the visible size and not the true volume changes.
[6] The confocal geometry of the Raman microscope excludes measuring the spectra from the liquid phase when focused on a crystal, therefore, the bands of the solvent could not belong to the pressure medium around the solid sample but were measured from the solvent inside the crystalline solvate.

pattern. Based on how the recrystallization proceeded, as well as on the volume of the unit cell of the first unknown phase and its Raman spectra, we find it most probable that this new phase is a solvate of L-alanine with one of the components of the pressure-transmitting liquid. For the second unknown phase there were diffraction patterns, but no Raman spectra. The unit-cell volume of the second phase is close to the unit-cell volume of L-alanine at the same pressure, but the cell parameters differ. This can be one more solvate of L-alanine, or a metastable phase of pure L-alanine, which forms only from a precursor. This needs further investigation, and the results of the structure solution of the two new phases will be reported later elsewhere.

To the best of our knowledge, no solvates of L-alanine have been described so far. At ambient conditions the solubility of L-alanine in methanol–ethanol (4:1), and also in methanol–ethanol–water (16:3:1), is extremely low. The solubility of L-alanine in water is known to grow with pressure increasing up to 0.35 GPa (data for higher pressures are not available; Matsuo *et al.*, 2002; Jit & Feng, 2008; Cibulka *et al.*, 2010). The effect of pressure on the solubility of L-alanine in alcohol–water mixtures has never been studied, although it is known that the addition of water to alcohols or *vice versa* has a strong effect on the solubility of amino acids at ambient pressure (Fuchs *et al.*, 2006). The increase in the polarization of the L-alanine zwitterions in the crystal with increasing pressure may be related to the increased interaction with solvent molecules. The interactions between L-alanine and various solvents at variable temperature–pressure conditions are definitely related to the possibility of solvate(s) formation and deserve further detailed studies.

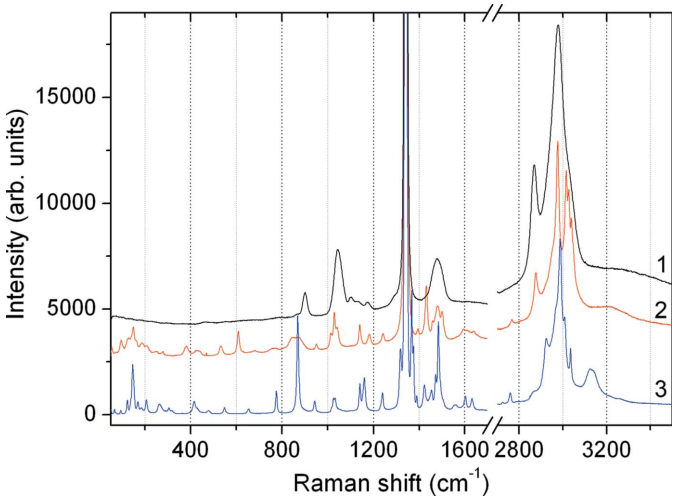

Figure 10
Raman spectra of the pressure-transmission medium (1), a new polycrystalline phase, the first 'solvate' (2), and the crystal of L-alanine (3) at the same pressure, 4.1 GPa.

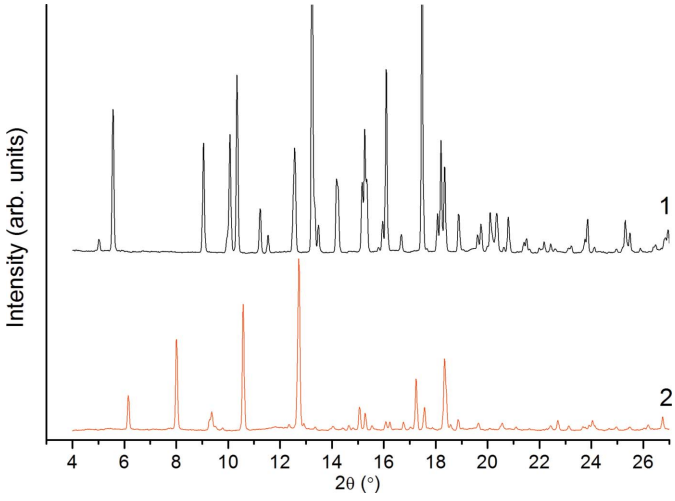

Figure 11
Powder diffraction patterns of new polycrystalline phases, first 'solvate' at 3.8 GPa (1), second 'solvate' at 1.1 GPa (2).

4. Conclusions

The studies on the effect of pressure on the crystalline amino acids provide examples of the extremely complex behavior of seemingly simple systems. The smallest chiral amino acid, L-alanine, is no exception. Although at 2 GPa the two cell parameters (*a* and *b*) become accidentally equal to each other, the space-group symmetry remains orthorhombic and no structural phase transitions have been detected at least up to 12.3 GPa. Pressure seems to favor a continuous shift of the H

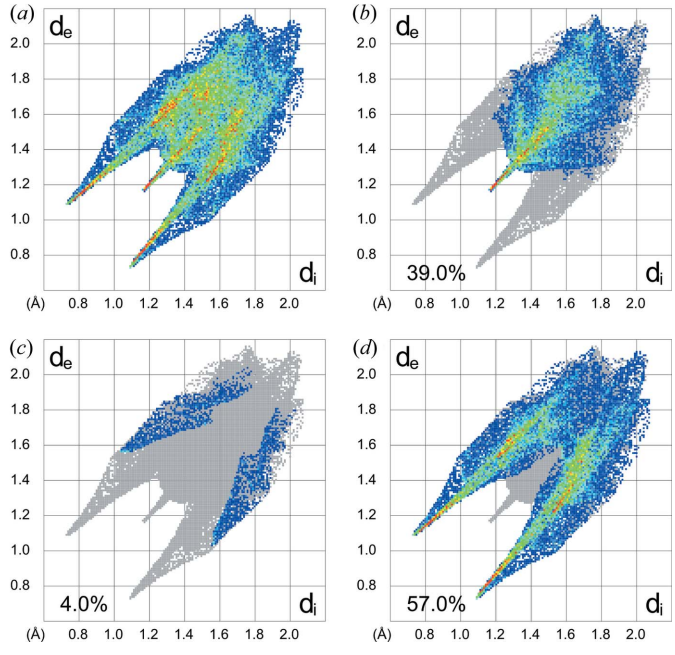

Figure 12
Two-dimensional Hirshfeld fingerprint plots of L-alanine at 0.2 GPa. (*a*) All contacts shown, (*b*) H—H contacts, (*c*) C—H contacts and (*d*) O—H contacts. The colour in the sequence white–blue–green–red is a summary of the frequency of each combination of d_e and d_i across the surface of a molecule (in increasing order), where d_i is the internal distance and d_e the external distance from the Hirshfeld surface to the nearest molecule. The features along the diagonal occur because of the H—H contacts, while the 'wings' are due to O—H and C—H interactions.

atom along the N*—H*···O* hydrogen bonds in the chain of L-alanine zwitterions from the O atom of one zwitterion to the N atom of another, so that by 2–3 GPa the two C—O bonds in a carboxylic group become much closer in length than they were at ambient pressure. The lattice dynamics of L-alanine are very sensitive to any changes in the properties of the hydrogen bonds. Therefore, it is no surprise that the low-wavenumber Raman spectra also change in the same pressure range, which was erroneously assumed to be a structural orthorhombic-to-tetragonal phase transition in previous publications. A combination of X-ray diffraction, Raman spectroscopy and optical microscopy turns out to be synergetic when studying the subtle pressure-induced changes in the molecular crystals. In this respect, it is worth noting that recently the phase transitions at 1.5 and 4.4 GPa, presumably with a symmetry change, have been reported for the completely deuterated L-alanine crystals, based on a Raman spectroscopy study (Gonçalves *et al.*, 2009). A careful diffraction experiment could distinguish between a structural polymorphic transformation and dynamic processes.

This work was supported by grants from BRHE (RUX0-008-NO-06), RFBR (08-03-00143, 09-03-00451), by the Integration Project Nos. 13 and 109 of the Siberian Branch of RAS, and the contract from FASI (RF) No. 02.740.11.5102; the single-crystal diffractometer and the Raman spectrometer have been purchased using money from the Innovation Project of Rosobrazovanie No. 456 (2007–2009). RQC is supported by an EPSRC Research Fellowship (EP/D0735X) to Paul F. McMillan at UCL. The DAC for the first series of synchrotron powder diffraction was kindly provided by Dr Ahsbahs, who has also given us much valuable practical advice on operating the cell. The friendly assistance of the Swiss–-Norwegian Beamline (SNBL) with the synchrotron radiation experiments is gratefully acknowledged. We thank Dr N. Casati, Dr K. Dziubek and Dr A. Budzianowski for valuable advice on technical aspects of single-crystal diffraction data collection and processing, and Professor P. Freire for providing us his primary experimental data for a comparative analysis.

References

Ahsbahs, H. (1996). *Z. Kristallogr.* **11**, 30.

Ahsbahs, H. (2004). *Z. Kristalogr.* **219**, 305–308.

Allan, D. R., Miletich, R. & Angel, R. J. (1996). *Rev. Sci. Instrum.* **67**, 840–844.

Angel, R. J. (2004). *J. Appl. Cryst.* **37**, 486–492.

Barthes, M., Bordallo, H. N., Drenoyer, F., Lorenzo, J.-E., Zaccaro, J., Robert, A. & Zontone, F. (2004). *Eur. Phys. J. B*, **37**, 375–382.

Boehler, R. (2006). *Rev. Sci. Instrum.* **77**, art. No. 115103.

Boldyreva, E. V. (2007*a*). *Models, Mysteries and Magic of Molecules*, edited by J. C. A. Boeyens & J. F. Ogilvie, pp. 69–194. Berlin: Springer Verlag.

Boldyreva, E. V. (2007*b*). *Cryst. Growth Des.* **7**, 1662–1668.

Boldyreva, E. V. (2007*c*). *Proceedings of the IVth International Conference on High Pressures Biosci. Biotechnology*, presented by J-STAGE, Tsukuba, Japan, 25–26 September 2006, edited by F. Abe & A. Suzuki, pp. 28–46. Saitama, Japan: Japan Science & Technology Agency.

Boldyreva, E. V. (2008). *Acta Cryst.* A**64**, 218–231.

Boldyreva, E. V. (2009). *Phase Transitions*, **82**, 303–321.

Boultif, A. & Louër, D. (2004). *J. Appl. Cryst.* **37**, 724–731.

Budzianowski, A. & Katrusiak, A. (2004). *High-Pressure Crystallography*, edited by A. Katrusiak & P. F. McMillan, pp. 101–112. Dordrecht: Kluwer Academic Publishers.

Casati, N. (2010). *High-Pressure Crystallography. Fundamentals and Applications*, edited by E. Boldyreva & P. Dera. In the press. Dordrecht: Springer.

Casati, N., Macchi, P. & Sironi, A. (2009). *Chem. Commun.* **19**, 2679–2681.

Cibulka, I., Hnědkovský, L. & Šedlbauer, J. (2010). *J. Chem. Thermodyn.* **42**, 198–207.

David, W. I. F., Shankland, K., van de Streek, J., Pidcock, E., Motherwell, W. D. S. & Cole, J. C. (2006). *J. Appl. Cryst.* **39**, 910–915.

Destro, R., Bianchi, R., Gatti, C. & Merati, F. (1991). *Chem. Phys. Lett.* **186**, 47–52.

Destro, R., Marsh, R. E. & Bianchi, R. (1988). *J. Phys. Chem.* **92**, 966–973.

Destro, R., Soave, R. & Barzaghi, M. (2008). *J. Phys. Chem. B*, **112**, 5163–5174.

Dunitz, J. D. & Ryan, R. R. (1966). *Acta Cryst.* **21**, 617–618.

Farrugia, L. J. (1999). *J. Appl. Cryst.* **32**, 837–838.

Forman, R. A., Piermarini, G. J., Dean Barnett, J. & Block, S. (1972). *Science*, **176**, 284–285.

Fuchs, D., Fischer, J., Tumakaka, F. & Sadowski, G. (2006). *Ind. Eng. Chem. Res.* **45**, 6578–6584.

Fujishiro, I., Piermarini, G. J., Block, S. & Munro, R. G. (1981). *High Pressure in Research and Industry, Proc. 8th AIRAPT Conf.*, Uppsala, edited by C. M. Backman, T. Johannison & L. Tegner, pp. 608–611.

Hammersley, A. P., Svensson, S. O., Hanfland, M., Fitch, A. N. & Häusermann, D. (1996). *High Pressure Res.* **14**, 235–248.

Gómez-Zavaglia, A. & Fausto, R. (2003). *Phys. Chem. Chem. Phys.* **5**, 3154–3161.

Gonçalves, R. O., Freire, P. T. C., Bordallo, H. N., Lima Jr, J. A., Melo, F. E. A., Mendes Filho, J., Argyriou, D. N. & Lima, R. J. C. (2009). *J. Raman Spectrosc.* **40**, 958–963.

Jit, P. & Feng, W. (2008). *Ind. Eng. Chem. Res.* **47**, 6275–6279.

Jönsson, P.-G. & Kvick, Å. (1972). *Acta Cryst.* B**28**, 1827–1833.

Katrusiak, A. (1990). *Acta Cryst.* B**46**, 246–256.

Katrusiak, A. (1991). *Cryst. Res. Technol.* **26**, 523–531.

Katrusiak, A. (1992). *J. Mol. Struct.* **269**, 329–354.

Katrusiak, A. (1993). *Phys. Rev. B*, **48**, 2992–3002.

Katrusiak, A. (1995). *Phys. Rev. B*, **51**, 589–592.

Katrusiak, A. (1996). *Crystallogr. Rev.* **5**, 133–180.

Katrusiak, A. (2001). *Frontiers of High Pressure Research II Application of High Pressure to Low-Dimensional Novel Electronic Materials*, edited by H. D. Hochheimer, B. Kuchta, P. K. Dorhout & J. F. Yarger, pp. 73–85. Dordrecht: Kluwer Academic Publishers.

Katrusiak, A. (2004). *High-Pressure Crystallography*, edited by A. Katrusiak & P. F. McMillan, pp. 513–520. Dordrecht: Kluwer Academic Publishers.

Katrusiak, A. (2010). *High-Pressure Crystallography. Fundamentals and Applications*, edited by E. Boldyreva & P. Dera. In the press. Berlin: Springer.

Kolesov, B. A. & Boldyreva, E. V. (2010*a*). *J. Raman Spectrosc.* **41**, 670–677.

Kolesov, B. A. & Boldyreva, E. V. (2010*b*). *J. Raman Spectrosc.* In the press.

Larson, A. C. & Von Dreele, R. B. (1994). *GSAS.* Report LAUR 86–748. Los Alamos National Laboratory, New Mexico, USA.

Lehmann, M. S., Koetzle, T. F. & Hamilton, W. C. (1972). *J. Am. Chem. Soc.* **94**, 2657–2660.

Macrae, C. F., Edgington, P. R., McCabe, P., Pidcock, E., Shields, G. P., Taylor, R., Towler, M. & van de Streek, J. (2006). *J. Appl. Cryst.* **39**, 453–457.

Martins, D. M. S., Middlemiss, D. S., Pulham, C. R., Wilson, C. C., Weller, M. T., Henry, P. F., Shankland, N., Shankland, K., Marshall, W. G., Ibberson, R. M., Knight, K., Moggach, S., Brunelli, M. & Morrison, C. A. (2009). *J. Am. Chem. Soc.* **131**, 3884–3893.
Matsuo, H., Suzuki, Y. & Sawamura, S. (2002). *Fluid Phase Equilib.* **200**, 227–237.
McKinnon, J. J., Jayatilaka, D. & Spackman, M. A. (2007). *Chem. Commun.* **37**, 3814–3816.
McKinnon, J. J., Spackman, M. A. & Mitchell, A. S. (2004). *Acta Cryst.* B**60**, 627–668.
Moggach, S. A., Parsons, S. & Wood, P. A. (2008). *Crystallogr. Rev.* **14**, 143–184.
Olsen, J. S., Gerward, L., Freire, P. T. C., Mendes Filho, J., Melo, F. E. A. & Souza Filho, A. G. (2008). *J. Phys. Chem. Solids*, **69**, 1641–1645.
Olsen, J. S., Gerward, L., Souza Filho, A. G., Freire, P. T. C., Mendes Filho, J. & Melo, F. E. A. (2006). *High Pressure Res.* **26**, 433–437.
Oxford Diffraction (2008*a*). *CrysAlisCCD*. Oxford Diffraction Ltd, Abingdon, England.
Oxford Diffraction (2008*b*). *CrysAlisRED*. Oxford Diffraction Ltd, Abingdon, England.
Peterson, M. A. & Nash, C. P. (1985). *J. Phys. Chem.* **89**, 522–524.
Piermarini, G. J., Block, S. & Barnett, J. D. (1973). *J. Appl. Phys.* **44**, 5377–5382.
Piermarini, G. J., Block, S., Barnett, J. D. & Forman, R. A. (1975). *J. Appl. Phys.* **46**, 2774–2780.
Sheldrick, G. M. (2008). *Acta Cryst.* A**64**, 112–122.
Sowa, H. & Ahsbahs, H. (2006). *J. Appl. Cryst.* **39**, 169–175.
Spek, A. L. (2009). *Acta Cryst.* D**65**, 148–155.
Stoe & Cie (2002). *WinXPOW*. Stoe & Cie GmbH, Darmstadt, Germany.
Teixeira, A. M. R., Freire, P. T. C., Moreno, A. J. D., Sasaki, J. M., Ayala, A. P., Mendes Filho, J. & Melo, F. E. A. (2000). *Solid State Commun.* **116**, 405–409.
Wilson, C. C. (2001). *Acta Cryst.* B**57**, 435–439.
Wilson, C. C., Myles, D., Ghosh, M., Johnson, L. N. & Wang, W. (2005). *New J. Chem.* **29**, 1318–1322.
Wolff, S. K., Grimwood, D. J., McKinnon, J. J., Jayatilaka, D. & Spackman, M. A. (2007). *CrystalExplorer*, Version 2.1, Technical Report. University of Western Australia, http://hirshfeldsurface-net.blogspot.com/.